José L. AZCUE-PUMA[1], Alfeu J. SGUAREZI FILHO[2], Ernesto RUPPERT[1]

Universidade Estadual de Campinas (1), Universidade Federal do ABC (2)

Fuzzy logic based vector control for three-phase induction motor

Abstract. *This article proposes a Takagi-Sugeno Fuzzy (TSF) controller for vector control method applied in three-phase induction motor control. The conventional vector control method has two PI current controllers. With the aim to reduce the quantity of these controllers, it is proposed a unique fuzzy controller to substitute both PI controllers. The performance of the proposed TSF controller is analyzed through several test. The simulation and experimental results show that the proposed TSF controller ensures decoupling current control and low current ripple, validating the TSF controller.*

Streszczenie. *W artykule zaproponowano metodę sterowania wektorowego trójfazowym silnikiem indukcyjnym z wykorzystaniem regulatora rozmytego Takagi-Sugeno zastępującego klasyczne regulatory PI. Przeprowadzono badania symulacyjne i eksperymentalne, weryfikujące skuteczność działania sterowania. (**Sterowanie wektorowe trójfazową maszyną indukcyjną z wykorzystaniem logiki rozmytej**).*

Keywords: Vector Control, Fuzzy Controllers, Induction Motor.
Słowa kluczowe: sterowanie wektorowe, regulator rozmyty, maszyna indukcyjna.

Introduction

The three-phase induction motors (IM) are widely used in industrial application, because of their simple and robust structure, higher torque-to-weight ratio, higher reliability and ability to operate in dangerous environment. However, because of the coupling between torque and flux, unlike dc motor, their control is a challenging task. A popular method to control the high performance electric drive for IM is the field oriented control (FOC) [1]. FOC leads to decoupling of stator current into torque and flux, producing components that give independent control over the motor torque while maintaining a constant flux that enables an accurate and precise IM control.

Fuzzy logic offers an alternative technique to the design of such a control systems making decisions based on human expertise, thus avoiding complex calculations. The Fuzzy Logic Controller (FLC) to be investigated in this article is the Sugeno's type [2], although there exist other types, for example, the Mamdani's [3] and the Yamakawa's [4].

Fuzzy controller have proved powerful in the power electronics area and control of electric machines as shown in various articles in the literature, e.g., in [5] and [6] are implemented a FLC for the speed control using FOC technique. It provides better motor control with high dynamic performance. In [7] another fuzzy speed controller is compared with conventional PI controller, shown that this controller takes superior performance under varying operating conditions, such as step change in speed and torque reference. Similarly, [8] proposes the fuzzy speed controller, but this controller is applied in indirect field-oriented control (IFOC) method. This method was compared with two speed control techniques, scalar control and conventional indirect field oriented control, showing its superiority. In [9] is proposed a neuro-fuzzy controller for speed control of an IM, it assures excellent performance but this method is also applied to IFOC method.

Radwan et al. [10] proposes the FLC with less computational process with aim to facilitate its real-time implementation, the FLC parameters were tuned by genetic algorithm resulting in a robust controller for high performance industrial drive applications, and [11] also is applied a genetic algorithms to optimize the fuzzy speed controller design with indirect FOC scheme. Besides, more controllers that works with self-organizing self-tuning fuzzy logic controller, and a speed model reference adaptive control are presented in [12] and [13, 14], respectively.

In [15] is investigates the effectiveness of the self-tuned FLC in the current control loop of IM drives based on FOC, its experimental results show better performance in comparison with the optimal PI current controllers. Although, this FLC has various parameters to be adjusted.

The majority of the articles cited above are focused on speed control, even when the current control plays an important role within the Direct Field Oriented Control (DFOC) method. Unlike the previously mentioned works, this article proposes a unique TSF controller in order to replace the both PI current controllers used in conventional DFOC method. The TSF controller calculates the quadrature components of the stator voltage vector represented in the rotor-flux-oriented reference frame. The inputs of the TSF controller are the direct-axis stator current error and the quadrature-axis stator current error. The rule base for the proposed TSF controller is defined as a function of its inputs. The membership functions used for the fuzzification of the TSF controller inputs have trapezoidal and triangular shapes, because these functions are suitable for real-time operations [16]. Therefore, the first output, it is the direct-axis component of the stator voltage vector, is represented as a linear combination of the TSF controller inputs. However, the quadrature-axis component of the stator voltage is similarly represented as a linear combination used in the first output but with the coefficients interchanged, not to be necessary another different coefficients values for this output, being only necessary to adjust two coefficients for each rule instead of four coefficients present in conventional DFOC method with two PI current controllers. The simulation and experimental results show that the proposed TSF controller for the DFOC method has a good performance when was test under various operating conditions, validating the proposed method.

Dynamical Equations of the Three-Phase Induction Motor

By the definition of the fluxes, currents and voltages space vectors, the dynamical equations of the three-phase IM in stationary reference frame can be put into the following mathematical form [17]:

$$\vec{u}_s = R_s\vec{i}_s + \frac{d\vec{\psi}_s}{dt} \tag{1}$$

$$0 = R_r\vec{i}_r + \frac{d\vec{\psi}_r}{dt} - j\omega_r\vec{\psi}_r \tag{2}$$

$$\vec{\psi}_s = L_s\vec{i}_s + L_m\vec{i}_r \tag{3}$$

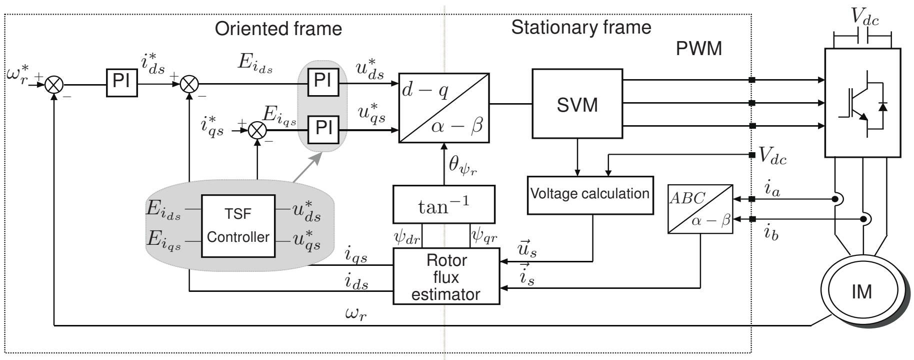

Fig. 1. Direct Field Oriented Control structure with TSF Controller.

$$\vec{\psi}_r = L_r\vec{i}_r + L_m\vec{i}_s \quad (4)$$

where $\vec{u}_s$ is the stator voltage space vector, $\vec{i}_s$ and $\vec{i}_r$ are the stator and rotor current space vectors, respectively, $\vec{\psi}_s$ and $\vec{\psi}_r$ are the stator and rotor flux space vectors, ω_r is the rotor angular speed, R_s and R_r are the stator and rotor resistances, L_s, L_r and L_m are the stator, rotor and mutual inductances, respectively.

The electromagnetic torque is expressed in terms of the cross-vectorial product of the stator and the rotor flux space vector.

$$t_e = \frac{3}{2}P\frac{L_m}{L_r}\vec{\psi}_r \times \vec{i}_s \quad (5)$$

$$t_e = \frac{3}{2}P\frac{L_m}{L_r}(\psi_{dr}i_{qs} - \psi_{qr}i_{ds}) \quad (6)$$

where P is a number of pole pairs, ψ_{dr} and ψ_{qr} are the quadrature components of the rotor flux, and i_{ds} and i_{qs} are the quadrature components of the stator current.

Direct Field Oriented Control

In rotor-flux-oriented reference frame the quadrature component of the rotor flux disappears and a physically easily comprehensible representation of the relations between torque, flux and current components are obtained. This representation can be expressed in the following formula.

$$\psi_{dr} = \frac{L_m}{1+sT_r}i_{ds} \quad (7)$$

$$t_e = \frac{3}{2}P\frac{L_m}{L_r}\psi_{dr}i_{qs} \quad (8)$$

Considering that $\psi_{dr} = \psi_{\mathbf{r}}$, we can rewrite this equation,

$$t_e = \frac{3}{2}P\frac{L_m}{L_r}\psi_{\mathbf{r}}i_{qs} \quad (9)$$

where s is a Laplace operator, $\psi_{\mathbf{r}}$ is the rotor flux module, and $T_r = L_r/R_r$ is a rotor time constant.

Equations (8) and (9) show that the component i_{ds} of the stator current can be used as a control quantity for the rotor flux ψ_{dr}. If the rotor flux can be kept constant with the help of i_{ds}, then the cross component i_{qs} plays the role of a control variable for the torque t_e [18].

The Proposed Direct Field Oriented Control Method

Figure 1 shows the block diagram of the proposed Direct Field Oriented Control (DFOC) method, it only needs sense the DC link voltage and the two phases of the stator currents of the three-phase IM to calculate the stator voltage and to estimate the rotor flux. In the DFOC method the TSF controller takes as inputs the direct-axis component of the stator current error ($E_{i_{ds}}$) and the quadrature-axis component of the stator current error ($E_{i_{qs}}$), and as outputs the quadrature components of the stator voltage necessary to maintain the speed and load. These outputs are represented in the rotor-flux-oriented reference frame. Details about the TSF controller are going to be presented in the next section.

Stator Voltage Calculation

The stator voltage calculation utilize the DC link voltage V_{dc}, and the inverter switch state (S_a, S_b, S_c) of the three leg two level inverter. The stator voltage vector $\vec{u}_s$ is determined as in [19],

$$\vec{u}_s = \frac{2}{3}\left[(S_a - \frac{S_b+S_c}{2}) + j\frac{\sqrt{3}}{2}(S_b - S_c)\right]V_{dc} \quad (10)$$

Rotor Flux Estimation

To estimate the rotor flux firstly we need to estimate the stator flux. The stator flux estimation depends of the back electromotive force (emf), it is:

$$\begin{aligned} \vec{\psi}_s &= \int(\vec{u}_s - R_s\cdot\vec{i}_s)dt \\ \vec{\psi}_s &= \int(\vec{\text{emf}})dt \end{aligned} \quad (11)$$

when the stator flux is calculated with equation (11) it has problems associated with a pure integrator. With the aim to solve this problem is used the integrator with an adaptive compensation method proposed in [20]. This method can be used to accurately estimate the motor flux including its magnitude and phase angle over a wide speed range.

Figure 2 shows a block diagram of this method. The main idea of this method is the fact that the motor flux is orthogonal to its back emf. The quadrature detector detect if the orthogonality between the estimated flux and bemf is maintained. A PI controller is used to generate a compensation level, it is

$$\psi_{\text{cmp}} = (k_p + \frac{k_i}{s})\frac{\psi_{qs}\cdot\text{emf}_q + \psi_{ds}\cdot\text{emf}_d}{|\vec{\psi}_s|} \quad (12)$$

where k_p and k_i are the gains of the PI controller. The magnitude of ψ_{cmp} is governed by equation (12). The operating principle of this method is explained by using a vector diagram shown in Figure 3. The estimated stator flux vector is a sum of two vectors, a feedforward vector $\vec{\psi}_1$ which is the output of the Low Pass (LP) filters (ψ_{d1} and ψ_{q1}) and a feedback vector $\vec{\psi}_2$ which is composed of ψ_{d2} and ψ_{q2}. Ideally, the flux vector $\vec{\psi}_s$ should be orthogonal to the $\vec{\mathrm{emf}}$, and the output of the quadrature detector is zero. When an initial value or dc drift is introduced to the integrator, the above orthogonal relation is lost, and the phase angle between the flux and emf vectors is no longer 90°, which yields an error signal defined by

$$\begin{aligned} \Delta\vec{e} &= \vec{\psi}_s \cdot \vec{\mathrm{emf}} / \left|\vec{\psi}_s\right| \\ &= (\psi_{qs} \cdot \mathrm{emf}_q + \psi_{ds} \cdot \mathrm{emf}_d) / \left|\vec{\psi}_s\right| \\ &= |\mathrm{emf}| \cos(\gamma) \end{aligned} \tag{13}$$

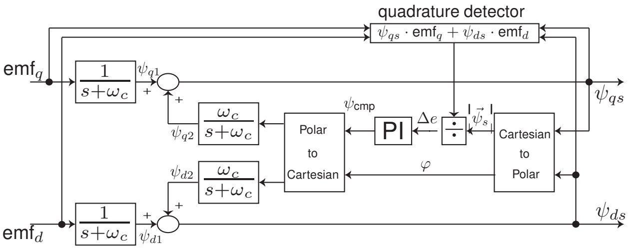

Fig. 2. Block diagram of the adaptive compensation method.

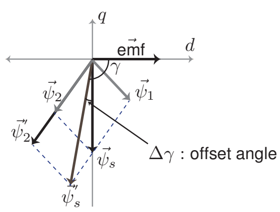

Fig. 3. Vector diagram showing the emf and flux linkage relationship.

Assuming that the magnitude of the feedback vector $\vec{\psi}_2$ is increased to $\vec{\psi}_2''$ as shown in Figure 3 due to a dc offset or initial value problem, the phase angle γ will be greater that 90°. The quadrature detector will generate a negative error signal. The output of the PI regulator ψ_{cmp} is reduced and so is the feedback vector. As a result, the flux vector $\vec{\psi}_s''$ moves toward the original position of 90° until the *orthogonal* relationship between $\vec{\psi}_s$ and $\vec{\mathrm{emf}}$ is reestablished. If γ is less than 90° for some reason, an opposite process will occur, which brings γ back to 90°. Therefore, the modified integrator with the adaptive control can adjust the flux compensation level ψ_{cmp} automatically to an optimal value such that the initial value and dc drift problems are essentially eliminated.

Remember that $\vec{\psi}_s = \psi_{ds} + j\psi_{qs}$, and with it the rotor flux $\vec{\psi}_r$ is calculated through motor model, in the stationary reference frame, as

$$\vec{\psi}_r = \frac{L_r}{L_m}\vec{\psi}_s - \frac{L_s L_r - L_m^2}{L_m}\vec{i}_s \tag{14}$$

The rotor flux angle θ_{ψ_r}, necessary to do the coordinate transformation of the system is calculated by

$$\theta_{\psi_r} = \tan^{-1}\left(\frac{\psi_{qr}}{\psi_{dr}}\right) \tag{15}$$

Takagi-Sugeno Fuzzy (TSF) Controller

The TSF controller [2] is based on a suitable set of fuzzy rules, carried out from both the knowledge of the experimental behavior and the internal structure of the controlled system. In order to design a TSF controller, the following steps must be performed:

1. development of a suitable rule set;
2. selection of input/output variables and their quantization in fuzzy sets;
3. definition of membership functions to be associated to the input variables;
4. selection of the defuzzification technique.

The TSF controller takes as inputs the direct-axis component of the stator current error $E_{i_{ds}}$ and the quadrature-axis component of the stator current error $E_{i_{qs}}$, and as outputs the quadrature components of the stator voltage vector. The output stator voltage is represented in the rotor-flux-oriented reference frame. The first output (u_{ds}^*) is a linear combination of the inputs, similarly, the second output (u_{qs}^*) takes the similar linear combination used in the first output but with the coefficients interchanged as is shown in Figure 4.

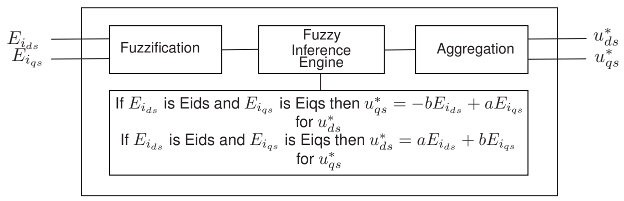

Fig. 4. The structure of a fuzzy logic current controller.

Membership Functions

The Membership Functions (MFs) of the TSF controller inputs are shown in Figure 5 and in Figure 6.

The universe of discourse for the input $E_{i_{ds}}$ is defined in the closed interval [-0.5, 0.5]. The extreme MFs have trapezoidal shapes but the middle MF takes triangular shape as it is shown in Figure 5. However, the universe of discourse for the input $E_{i_{qs}}$ is defined in the closed interval [-10, 10] as is shown in Figure 6. The shapes of these MFs are similar to the first input. For both inputs the linguistic labels are N, Ze and P that means Negative, Zero and Positive, respectively.

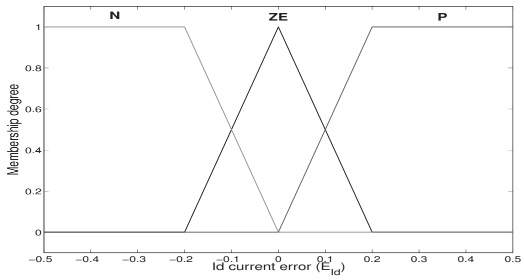

Fig. 5. Membership function for the direct-axis component of the stator current error $E_{i_{ds}}$.

The Fuzzy Rule Base

A set of rules for the direct component of the stator voltage u_{ds}^* are defined by the rules of the following form:

Table 1. Fuzzy rules for computation of u^*_{ds} and u^*_{qs}.

$\mathbf{E_{i_{ds}}}$ / $\mathbf{E_{i_{qs}}}$	N	ZE	P
N	$V_{ds}^{R_1} = a \cdot E_{i_{ds}} + b \cdot E_{i_{qs}}$ $V_{qs}^{R_1} = -b \cdot E_{i_{ds}} + a \cdot E_{i_{qs}}$	$V_{ds}^{R_2} = a \cdot E_{i_{ds}} + b \cdot E_{i_{qs}}$ $V_{qs}^{R_2} = -b \cdot E_{i_{ds}} + a \cdot E_{i_{qs}}$	$V_{ds}^{R_3} = c \cdot E_{i_{ds}} + d \cdot E_{i_{qs}}$ $V_{qs}^{R_3} = -d \cdot E_{i_{ds}} + c \cdot E_{i_{qs}}$
ZE	$V_{ds}^{R_4} = a \cdot E_{i_{ds}} + b \cdot E_{i_{qs}}$ $V_{qs}^{R_4} = -b \cdot E_{i_{ds}} + a \cdot E_{i_{qs}}$	$V_{ds}^{R_5} = c \cdot E_{i_{ds}} + d \cdot E_{i_{qs}}$ $V_{qs}^{R_5} = -d \cdot E_{i_{ds}} + c \cdot E_{i_{qs}}$	$V_{ds}^{R_6} = e \cdot E_{i_{ds}} + f \cdot E_{i_{qs}}$ $V_{qs}^{R_6} = -f \cdot E_{i_{ds}} + e \cdot E_{i_{qs}}$
P	$V_{ds}^{R_7} = c \cdot E_{i_{ds}} + d \cdot E_{i_{qs}}$ $V_{qs}^{R_7} = -d \cdot E_{i_{ds}} + c \cdot E_{i_{qs}}$	$V_{ds}^{R_8} = e \cdot E_{i_{ds}} + f \cdot E_{i_{qs}}$ $V_{qs}^{R_8} = -f \cdot E_{i_{ds}} + e \cdot E_{i_{qs}}$	$V_{ds}^{R_9} = e \cdot E_{i_{ds}} + f \cdot E_{i_{qs}}$ $V_{qs}^{R_9} = -f \cdot E_{i_{ds}} + e \cdot E_{i_{qs}}$

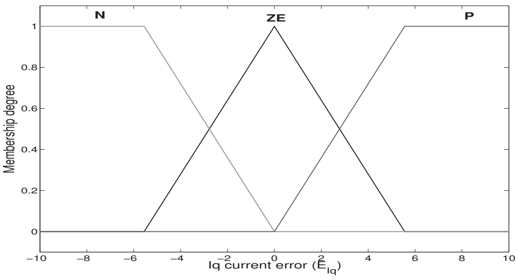

Fig. 6. Membership function for the quadrature-axis component of the stator current error $E_{i_{qs}}$.

$$R^1_{V_{ds}} \quad : \quad \text{if } E_{i_{ds}} \text{ is N and } E_{i_{qs}} \text{ is N then} \quad V_{ds}^{R_1} = a \cdot E_{i_{ds}} + b \cdot E_{i_{qs}}$$

However, the set of rules for the quadrature component of the stator voltage u^*_{qs} are defined by the rules of the following form:

$$R^1_{V_{qs}} \quad : \quad \text{if } E_{i_{ds}} \text{ is N and } E_{i_{qs}} \text{ is N then} \quad V_{qs}^{R_1} = -b \cdot E_{i_{ds}} + a \cdot E_{i_{qs}}$$

The *a* and *b* coefficients of the first-order polynomial function typically present in the consequent part of the firs-order Takagi-Sugeno fuzzy controllers. Observe that these coefficients for $V_{ds}^{R_1}$ and $V_{qs}^{R_1}$ are the same but with interchanged order, being it not necessary other different coefficients for each one, as they are repeated for all the rules. For instance, when the consequent part of the rule is a real number, we have a zero-order controller, but if the consequent is a linear combination we have a first-order controller [21]. The complete rule base to calculate u^*_{ds} and u^*_{qs} is shown in Table 1, where (a=5; b=0.1), (c=6.5; d=0.2), (e=8; f=0.1). The shape and the universe of discourse of the MFs and these coefficients were adjusted through the simulation process using the trial and error method.

Inference Method

In general, operators on fuzzy sets use triangular norms, which may be divided into T-norms (AND operators) and S-norms (OR operators) [22]. T-norms perform an intersection operation on fuzzy sets and have a particular importance in fuzzy logic control. T-norm is usually denoted as T (a,b). The T-norms used in our TSF controller is the product defined as:

$$\text{(16)} \quad \mu^{R_i} = T(\mu^i_{E_{i_{ds}}}, \mu^i_{E_{i_{qs}}}) \; = \; \mu^i_{E_{i_{ds}}} \cdot \mu^i_{E_{i_{qs}}} \quad \text{for} \quad i = 1, ..., n; \quad n = 9$$

where $\mu^i_{E_{i_{ds}}}$ and $\mu^i_{E_{i_{qs}}}$ are MFs degrees of the first and second TSF controller inputs, respectively, and μ^{R_i} is the truth value of the preposition.

Aggregation

The final output value u^*_{ds} inferred from $n = 9$ implications is aggregated as the average of all $V_{ds}^{R_i}$ with the weights μ^{R_i}:

$$\text{(17)} \qquad u^*_{ds} = \frac{\Sigma^n_{i=1} \mu^{R_i} V_{ds}^{R_i}}{\Sigma^n_{i=1} V_{ds}^{R_i}}$$

and the final output value u^*_{qs} inferred from $n = 9$ implications is aggregated as the average of all $V_{qs}^{R_i}$ with the weights μ^{R_i}:

$$\text{(18)} \qquad u^*_{qs} = \frac{\Sigma^n_{i=1} \mu^{R_i} V_{qs}^{R_i}}{\Sigma^n_{i=1} V_{qs}^{R_i}}$$

In our TSF controller, that is Sugeno type, it is not necessary the defuzzification interface [23]. This is so because, in Takagi-Sugeno fuzzy controllers, each rule is already crisp and the total result is determined by the weighted sum of each rule, as is shown in equations (17) and (18). The TSF controller was programmed in C programming language for the simulation because it facilitates its implementation in the digital signal processor TMS320F28335 from the Texas Instrument.

Simulations and Experimental Results

The simulations activities were performed using MATLAB R2011b simulation package together with Simulink block sets and fuzzy logic toolbox. The switching frequency of the three-phase two level inverter was set to be 10kHz, the direct component of the stator current (i^*_{ds}) was set to be 1.0 pu.

The experimental activities are realized with electronic circuits and three-phase IM. The experimental set-up consists of a DSP (Texas Instruments TMS320F28335) connected to a three-phase squirrel cage IM, driven by a 12kVA Semikron three-phase inverter (SKS 32F B6U+E1CIF+B6CI 12 V06). The mechanical load is imposed by a Foucault braking system. Conditioning signal boards are necessary to acquire the motor currents and the Dc link voltage from a high level of voltage and current to an appropriate voltage level to be sampled and converted by the internal AD converter.

In order to investigate the effectiveness of the proposed control system and in order to check the closed-loop stability of the complete system, we performed several tests. The simulated scenarios shown in this article covers the following situations: trapezoidal profile reversion, triangular profile reversion and step change in speed reference, the three tests were made with no-load. Besides, the step change in the motor load (from 0 to 1.0 pu and from 0 to 0.5 pu) at forty percent of rated speed was made. The parameters of the three-phase IM under test is shown in the appendix section.

Figure 7(a) shows the response of rotor angular speed when a trapezoidal profile reversion was applied to the motor with no-load. In this test the rotor speed tracked the reference as expected. Similar behavior is observed in experimental

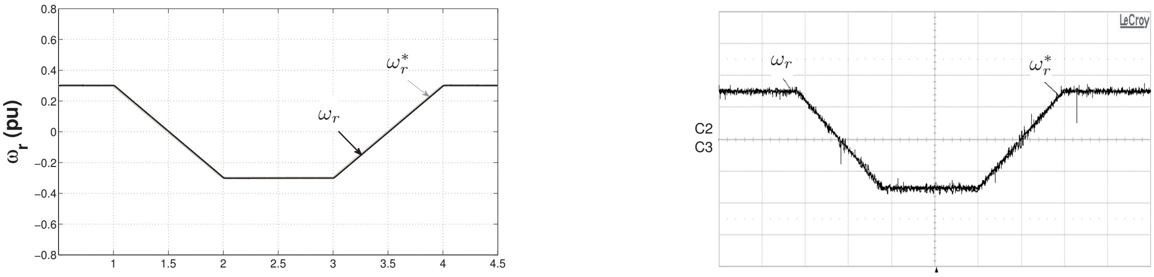

Fig. 7. Simulation (a) and Experimental (b) results of ω_r when trapezoidal profile reversion is applied with no-load (C2,C3: 0.2 pu/div, 5s/div).

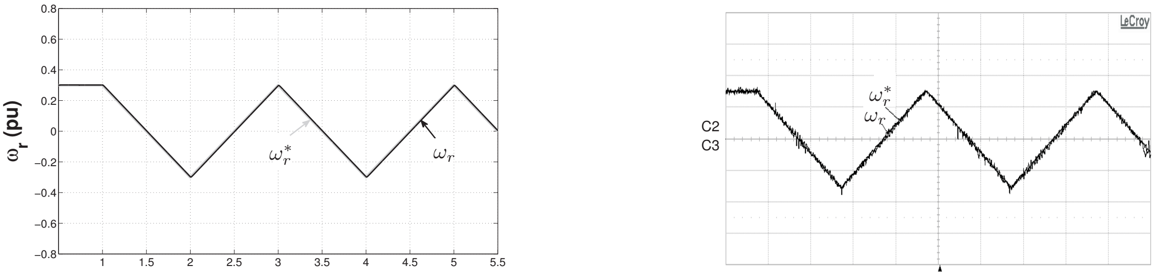

Fig. 8. Simulation (a) and Experimental (b) results of ω_r when triangular profile reversion is applied with no-load (C2,C3: 0.2 pu/div, 5s/div).

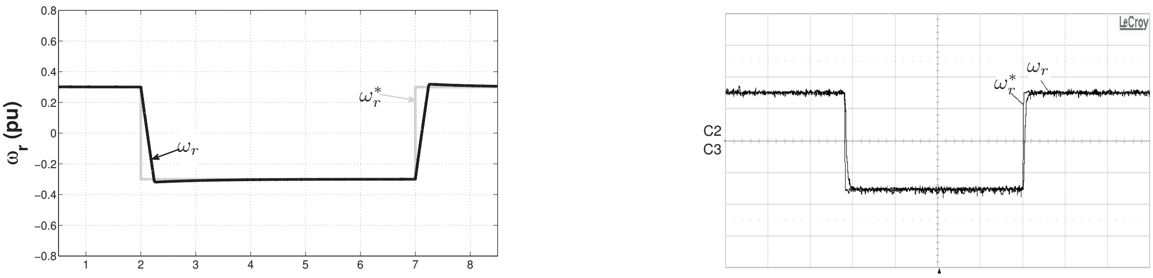

Fig. 9. Simulation (a) and Experimental (b) results of ω_r when step change in the speed reference is applied with no-load (C2,C3: 0.2 pu/div, 5s/div).

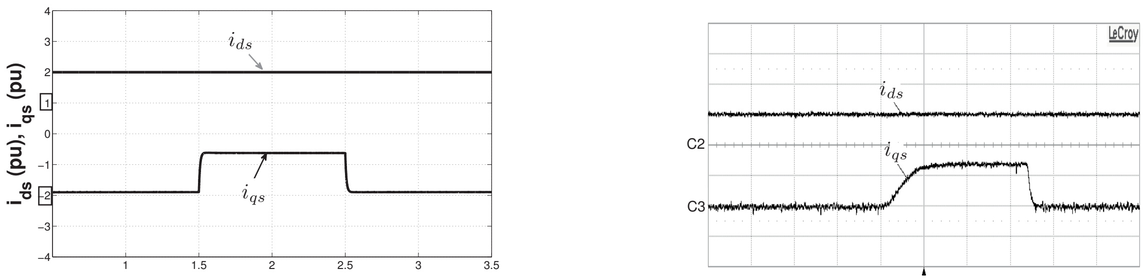

Fig. 10. Simulation (a) and Experimental (b) results of i_{ds} and i_{qs} when the rated load is applied (C2,C3: 0.5 pu/div, 5s/div).

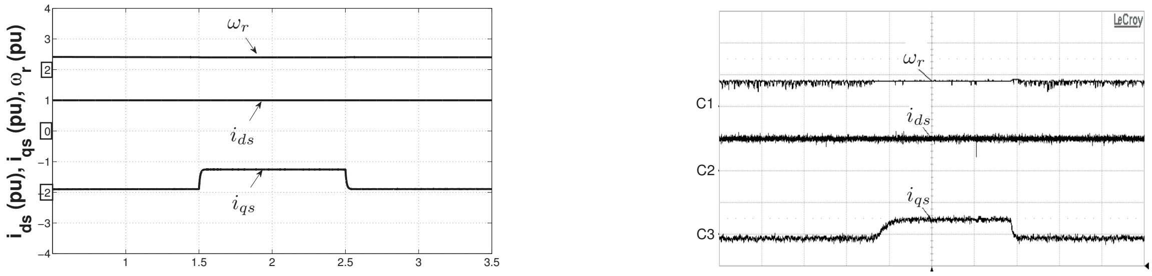

Fig. 11. Simulation (a) and Experimental (b) results of ω_r and, i_{ds} and i_{qs} when the 0.5 pu of rated load is applied (C1,C3: 0.5 pu/div; C2: 1 pu/div; 5s/div).

test as is shown in Figure 7(b). Although with some oscillations, the rotor angular speed tracked the reference speed very close and it was able to follow the rotor speed within 2% accuracy most of the time.

Figure 8(a) shows the response of rotor angular speed when triangular profile reversion was applied to the motor. This test was made with no-load too, the rotor speed tracked the triangular profile reference as expected. Similar behavior is observed in experimental test as is shown in Figure 8(b).

Figure 9(a) and Figure 9(b) show the simulation and experimental results of the rotor angular speed ω_r when a step change is imposed in the reference speed from 0.3 pu to -0.3 pu with no-load. The rotor angular speed achieves the reference speed at about 0.7 seconds.

Figure 10(a) and Figure 10(b) show the simulation and experimental results of the current components when the step change in the motor load is applied (from 0 to 1.0 pu). The quadrature-axis component of the stator current increase to maintain the load. Also, it is possible to observe a constant behavior of the direct-axis component of the stator current when load is applied, it shows the decoupled behavior of the DFOC method with the proposed TSF controller.

Finally, Figure 11(a) and Figure 11(b) show the simulation and experimental results of the current components and rotor angular speed when the step change in the motor load is applied (from 0 to 0.5pu). The behavior of quadrature components of the stator currents is as expected. When the load is applied the speed is maintained stable with a small overshoot when the load is retreat. All test results show a good performance of the proposed DFOC method with the proposed TSF controller.

Conclusion

In this article it is presented the DFOC method with TSF controller for the three-phase IM. The proposed controller substitutes the both PI current controllers present in conventional DFOC method. The TSF controller calculates the reference quadrature components of the stator voltage vector in rotor-flux-oriented reference frame. The rule base for the proposed TSF controller is defined as a function of the stator current error components. Constant switching frequency and low current ripple were obtained using space vector modulation technique. Numerical simulations and experimental test have been carried out at different operating conditions. These results show that the proposed DFOC scheme with TSF controller achieves a good performance as expected. It shows decoupling current control and low current ripple.

Appendix

The three-phase induction motor parameters are: rated voltage 220V/60Hz; rated Power 1.5 HP; rated torque 6.1 Nm; rated speed 180.12 rad/s; $R_s = 5.56\Omega$, $R_r = 4.25\Omega$; $L_s = L_r = 0.309$ H; $L_m = 0.296$ H; $J = 0.02K_g m^2$, $P = 2$ pole pairs.

REFERENCES

[1] F. Blaschke. The principle of field orientation as applied to the new transvector closed-loop control system for rotating field machines. *Siemens Review*, 39(no 5):pp. 217–220, May 1972.

[2] T. Takagi and M. Sugeno. Fuzzy identification of systems and its applications to modeling and control. *IEEE transactions on systems, man, and cybernetics*, 14(no. 1):pp. 116–132, Jan/Feb 1985.

[3] E. H. Mamdani. Application of fuzzy logic algorithms for control of simple dynamic plant. *IEEE Proceedings of the Institution of Electrical Engineers*, 121(no. 12):pp 1585–1588, 1974.

[4] T. Yamakawa. Fuzzy controller hardware system. In *Proceedings of 2nd IFSA Congress*, pages pp. 827–830, 1987.

[5] V. Chitra and R. S. Prabhakar. Induction motor speed control using fuzzy logic controller. In *World Academy of Science, Engineering and Technology*, 2006.

[6] B. Heber, Longya Xu, and Y. Tang. Fuzzy logic enhanced speed control of an indirect field-oriented induction machine drive. *Power Electronics, IEEE Transactions on*, 12(5):772 – 778, sep 1997.

[7] Lee Hakju, Lee Jaedo, and Seong Sejin. Approach to fuzzy control of an indirect field-oriented induction motor drives. In *Industrial Electronics, 2001. Proceedings. ISIE 2001. IEEE International Symposium on*, volume 2, pages 1119 –1123 vol.2, 2001.

[8] B.M. Badr, A.M. Eltamaly, and A.I. Alolah. Fuzzy controller for three phases induction motor drives. In *Vehicle Power and Propulsion Conference (VPPC), 2010 IEEE*, pages 1 –6, sept. 2010.

[9] A. Mechernene, M. Zerikat, and S. Chekroun. Indirect field oriented adaptive control of induction motor based on neuro-fuzzy controller. In *Control Automation (MED), 2010 18th Mediterranean Conference on*, pages 1109 –1114, june 2010.

[10] T.S. Radwan, M.N. Uddin, and M.A. Rahman. A new and simple structure of fuzzy logic based indirect field oriented control of induction motor drives. In *Power Electronics Specialists Conference, 2004. PESC 04. 2004 IEEE 35th Annual*, volume 5, pages 3290 – 3294 Vol.5, june 2004.

[11] Moulay Rachid Douiri, Mohamed Cherkaoui, and Ahmed Essadki. Genetic algorithms based fuzzy speed controllers for indirect field oriented control of induction motor drive. *INTERNATIONAL JOURNAL OF CIRCUITS, SYSTEMS AND SIGNAL PROCESSING*, 6(no. 1):pp. 21–28, 2012.

[12] F. Ashrafzadeh, E.P. Nowicki, and J.C. Salmon. A self-organizing and self-tuning fuzzy logic controller for field oriented control of induction motor drives. In *Industry Applications Conference, 1995. Thirtieth IAS Annual Meeting, IAS '95., Conference Record of the 1995 IEEE*, volume 2, pages 1656 –1662 vol.2, oct 1995.

[13] E. Cerruto, A. Consoli, A. Raciti, and A. Testa. Fuzzy adaptive vector control of induction motor drives. *Power Electronics, IEEE Transactions on*, 12(6):1028 –1040, nov 1997.

[14] T. Orlowska-Kowalska and M. Dybkowski. Performance analysis of the sensorless adaptive sliding-mode neuro-fuzzy control of the induction motor drive with mras-type speed estimator. *BULLETIN OF THE POLISH ACADEMY OF SCIENCES*, 60:pp. 1–10, 2012.

[15] F. Profumo, G. Griva, and V. Donescu. Self tuning fuzzy logic current control for high performance induction motor drives. In *Industrial Electronics Society, 1998. IECON '98. Proceedings of the 24th Annual Conference of the IEEE*, volume 3, pages 1871 –1876 vol.3, aug-4 sep 1998.

[16] Prade H. Dubois, D. and R. (Eds.) Yager. *Fuzzy Sets for Intelligent Systems*. Morgan Kaufmann Publishers; 1st edition (August 1993), 1993.

[17] Peter Vas. *Sensorless vector and Direct Torque Control*. Oxford University Press, 1998.

[18] N.P. Quang and J.A. Dittrich. *Vector Control of Three-Phase AC Machines*. Springer, 2008.

[19] M. Bertoluzzo, G. Buja, and R. Menis. A direct torque control scheme for induction motor drives using the current model flux estimation. *Diagnostics for Electric Machines, Power Electronics and Drives, 2007. SDEMPED 2007. IEEE International Symposium on*, pages 185 –190, sept. 2007.

[20] Jun Hu and Bin Wu. New integration algorithms for estimating motor flux over a wide speed range. *Power Electronics, IEEE Transactions on*, 13(5):969 –977, sep 1998.

[21] Witold Pedrycz and Fernando Gomide. *Fuzzy Systems Engineering Toward Human-Centric Computing*. Wiley-IEEE Press, 2007.

[22] M.M. Gupta and J. Qi. Theory of t-norms and fuzzy inference methods. *Fuzzy Sets and Systems*, 40(3):431 – 450, 1991.

[23] D. Driankov, H. Hellendoorn, and M. Reinfrank. *An Introduction to Fuzzy Control*. Springer, 2nd. edition, 1996.

Authors: *M.Sc. José L. Azcue-Puma, Prof. Dr. Ernesto Ruppert, DSCE/FEEC/UNICAMP, Campinas - SP - Brazil, email: azcue@ieee.org, ruppert@fee.unicamp.br, Prof. Dr. Alfeu J. Sguarezi Filho, CECS/UFABC, Santo André - SP - Brazil, email: alfeu.sguarezi@ufabc.edu.br*